Research Article | Vol. 7, No. 7 | 1 Jul 2017 | OPTICAL MATERIALS EXPRESS 2571
Optical Materials EXPRESS

Laser spectroscopy of NV- and NV0 colour centres in synthetic diamond

ELISABETH FRACZEK,[1] VASILI G. SAVITSKI,[1,*] MATTHEW DALE,[2] BEN G. BREEZE,[2] PHIL DIGGLE,[2] MATTHEW MARKHAM,[3] ANDREW BENNETT,[3] HARPREET DHILLON,[3] MARK E. NEWTON,[2] AND ALAN J. KEMP[1]

[1]*Institute of Photonics, Department of Physics, University of Strathclyde, Glasgow, G1 1RD, UK*
[2]*Department of Physics, University of Warwick, Coventry, CV4 7AL, UK*
[3]*Element Six (UK) Limited, Global Innovation Centre, Harwell Campus, Oxfordshire, UK*
**vasili.savitski@strath.ac.uk*

Abstract: In this paper, we analyse the prospects for using nitrogen-vacancy centre (NV) containing diamond as a laser gain material by measuring its key laser related parameters. Synthetic chemical vapour deposition grown diamond samples with an NV concentration of ~1 ppm have been selected because of their relatively high NV concentration and low background absorption in comparison to other samples available to us. For the samples measured, the luminescence lifetimes of the NV- and NV0 centres were measured to be 8 ± 1 ns and 20 ± 1 ns, respectively. The respective peak stimulated emission cross-sections were $(3.6 \pm 0.1) \times 10^{-17}$ cm^2 and $(1.7 \pm 0.1) \times 10^{-17}$ cm^2. These measurements were combined with absorption measurements to calculate the gain spectra for NV- and NV0 for differing inversion levels. Such calculations indicate that gains approaching those required for laser operation may be possible with one of the samples tested and for the NV- centre.

OCIS codes: (140.1700) Color center lasers; (140.3380) Laser materials; (300.6360) Spectroscopy, laser.

References and links

1. R. S. Balmer, J. R. Brandon, S. L. Clewes, H. K. Dhillon, J. M. Dodson, I. Friel, P. N. Inglis, T. D. Madgwick, M. L. Markham, T. P. Mollart, N. Perkins, G. A. Scarsbrook, D. J. Twitchen, A. J. Whitehead, J. J. Wilman, and S. M. Woollard, "Chemical vapour deposition synthetic diamond: materials, technology and applications," J. Phys. Condens. Matter **21**(36), 364221 (2009).
2. I. Friel, S. L. Clewes, H. K. Dhillon, N. Perkins, D. J. Twitchen, and G. A. Scarsbrook, "Control of surface and bulk crystalline quality in single crystal diamond grown by chemical vapour deposition," Diamond Related Materials **18**(5-8), 808–815 (2009).
3. G. Davies, *Properties and growth of diamond*, Datareviews series (INSPEC, UK, 1994), Vol. 9.
4. R. P. Mildren and J. R. Rabeau, *Optical Engineering of Diamond* (Wiley-VCH Verlag GmbH & Co, 2013).
5. I. Aharonovich, A. D. Greentree, and S. Prawer, "Diamond photonics," Nat. Photonics **5**(7), 397–405 (2011).
6. A. J. Kemp, J. M. Hopkins, A. J. Maclean, N. Schulz, M. Rattunde, J. Wagner, and D. Burns, "Thermal Management in 2.3- µm Semiconductor Disk Lasers: A Finite Element Analysis," IEEE J. Quantum Electron. **44**(2), 125–135 (2008).
7. V. G. Savitski, I. Friel, J. E. Hastie, M. D. Dawson, D. Burns, and A. J. Kemp, "Characterization of Single-Crystal Synthetic Diamond for Multi-Watt Continuous-Wave Raman Lasers," IEEE J. Quantum Electron. **48**(3), 328–337 (2012).
8. R. J. Williams, J. Nold, M. Strecker, O. Kitzler, A. McKay, T. Schreiber, and R. P. Mildren, "Efficient Raman frequency conversion of high-power fiber lasers in diamond," Laser Photonics Rev. **9**(4), 405–411 (2015).
9. M. M. Biener, J. Biener, S. O. Kucheyev, Y. M. Wang, B. El-Dasher, N. E. Teslich, A. V. Hamza, H. Obloh, W. Mueller-Sebert, M. Wolfer, T. Fuchs, M. Grimm, A. Kriele, and C. Wild, "Controlled incorporation of mid-to-high Z transition metals in CVD diamond," Diamond Related Materials **19**(5-6), 643–647 (2010).
10. K. D. Jamison and H. K. Schmidt, "Doped diamond laser," US5504767 A (1996).
11. A. M. Zaitsev, *Optical Properties of Diamond: A Data Handbook* (Springer, 2001).
12. S. C. Rand and L. G. Deshazer, "Visible color-center laser in diamond," Opt. Lett. **10**(10), 481–483 (1985).
13. W. V. Smith, P. P. Sorokin, I. L. Gelles, and G. J. Lasher, "Electron-Spin Resonance of Nitrogen Donors in Diamond," Phys. Rev. **115**(6), 1546–1552 (1959).
14. F. Jelezko and J. Wrachtrup, "Single defect centres in diamond: A review," Phys. Status Solidi **203**(13), 3207–3225 (2006).

#294776 https://doi.org/10.1364/OME.7.002571
Journal © 2017 Received 28 Apr 2017; revised 2 Jun 2017; accepted 6 Jun 2017; published 22 Jun 2017

Optical Materials EXPRESS

15. M. W. Doherty, N. B. Manson, P. Delaney, F. Jelezko, J. Wrachtrup, and L. C. L. Hollenberg, "The nitrogen-vacancy colour centre in diamond," Phys. Rep. **528**(1), 1–45 (2013).
16. I. Aharonovich and S. Prawer, *Quantum Information Processing with Diamond. Principles and Applications.*, Woodhead Publishing Series in Electronic and Optical Materials (Elsevier, 2014).
17. A. Faraon, C. M. Santori, and R. G. Beausoleil, "Color centers affected by magnetic fields to produce light based on lasing," US20140072008 A1 (2014).
18. J. Jeske, J. H. Cole, and A. D. Greentree, "Laser threshold magnetometry," New J. Phys. **18**(1), 013015 (2016).
19. J. Jeske, D. W. M. Lau, X. Vidal, L. P. McGuinness, P. Reineck, B. C. Johnson, M. W. Doherty, J. C. McCallum, S. Onoda, F. Jelezko, T. Ohshima, T. Volz, J. H. Cole, B. C. Gibson, and A. D. Greentree, "Stimulated emission from nitrogen-vacancy centres in diamond," Nat. Commun. **8**, 14000 (2017).
20. S. Rand, "Synthetic Diamond for Color Center Lasers," in *Advanced Solid State Lasers*, OSA Technical Digest (Optical Society of America, 1986), FA9.
21. V. G. Vins and E. V. Pestryakov, "Color centers in diamond crystals: Their potential use in tunable and femtosecond lasers," Diamond Related Materials **15**(4-8), 569–571 (2006).
22. C. M. Breeding and J. E. Shigley, "The 'type' classification system of diamonds and its importance in gemology," Gems & Gemology **45**(2), 96–111 (2009).
23. T.-L. Wee, Y.-K. Tzeng, C.-C. Han, H.-C. Chang, W. Fann, J.-H. Hsu, K.-M. Chen, and Y.-C. Yu, "Two-photon Excited Fluorescence of Nitrogen-Vacancy Centers in Proton-Irradiated Type Ib Diamond," J. Phys. Chem. A **111**(38), 9379–9386 (2007).
24. T. Yamamoto, T. Umeda, K. Watanabe, S. Onoda, M. L. Markham, D. J. Twitchen, B. Naydenov, L. P. McGuinness, T. Teraji, S. Koizumi, F. Dolde, H. Fedder, J. Honert, J. Wrachtrup, T. Ohshima, F. Jelezko, and J. Isoya, "Extending spin coherence times of diamond qubits by high-temperature annealing," Phys. Rev. B **88**(7), 075206 (2013).
25. Y. Chu, N. P. de Leon, B. J. Shields, B. Hausmann, R. Evans, E. Togan, M. J. Burek, M. Markham, A. Stacey, A. S. Zibrov, A. Yacoby, D. J. Twitchen, M. Loncar, H. Park, P. Maletinsky, and M. D. Lukin, "Coherent Optical Transitions in Implanted Nitrogen Vacancy Centers," Nano Lett. **14**(4), 1982–1986 (2014).
26. G. Davies, "Current problems in diamond: towards a quantitative understanding," Physica B **273–274**, 15–23 (1999).
27. S. C. Lawson, D. Fisher, D. C. Hunt, and M. E. Newton, "On the existence of positively charged single-substitutional nitrogen in diamond," J. Phys. Condens. Matter **10**(27), 6171–6180 (1998).
28. C. D. Clark, R. W. Ditchburn, and H. B. Dyer, "The Absorption Spectra of Natural and Irradiated Diamonds," Proc. R. Soc. Lond. A Math. Phys. Sci. **234**(1198), 363–381 (1956).
29. G. Davies and M. F. Hamer, "Optical Studies of the 1.945 eV Vibronic Band in Diamond," Proc. R. Soc. Lond. A Math. Phys. Sci. **348**(1653), 285–298 (1976).
30. A. T. Collins and I. Kiflawi, "The annealing of radiation damage in type Ia diamond," J. Phys. Condens. Matter **21**(36), 364209 (2009).
31. T. Gaebel, M. Domhan, C. Wittmann, I. Popa, F. Jelezko, J. Rabeau, A. Greentree, S. Prawer, E. Trajkov, P. R. Hemmer, and J. Wrachtrup, "Photochromism in single nitrogen-vacancy defect in diamond," Appl. Phys. B **82**(2), 243–246 (2006).
32. B. Campbell and A. Mainwood, "Radiation Damage of Diamond by Electron and Gamma Irradiation," physica status solidi (a) **181**, 99–107 (2000).
33. F. C. Waldermann, P. Olivero, J. Nunn, K. Surmacz, Z. Y. Wang, D. Jaksch, R. A. Taylor, I. A. Walmsley, M. Draganski, P. Reichart, A. D. Greentree, D. N. Jamieson, and S. Prawer, "Creating diamond color centers for quantum optical applications," Diamond Related Materials **16**(11), 1887–1895 (2007).
34. V. M. Acosta, E. Bauch, M. P. Ledbetter, C. Santori, K. M. C. Fu, P. E. Barclay, R. G. Beausoleil, H. Linget, J. F. Roch, F. Treussart, S. Chemerisov, W. Gawlik, and D. Budker, "Diamonds with a high density of nitrogen-vacancy centers for magnetometry applications," Phys. Rev. B **80**(11), 115202 (2009).
35. S. Pezzagna, D. Rogalla, D. Wildanger, J. Meijer, and A. Zaitsev, "Creation and nature of optical centres in diamond for single-photon emission—overview and critical remarks," New J. Phys. **13**(3), 035024 (2011).
36. J. Walker, "Optical-Absorption and Luminescence in Diamond," Rep. Prog. Phys. **42**(10), 1605–1659 (1979).
37. G. A. Crosby and J. N. Demas, "Measurement of photoluminescence quantum yields. Review," J. Phys. Chem. **75**(8), 991–1024 (1971).
38. T.-S. Ahn, R. O. Al-Kaysi, A. M. Müller, K. M. Wentz, and C. J. Bardeen, "Self-absorption correction for solid-state photoluminescence quantum yields obtained from integrating sphere measurements," Rev. Sci. Instrum. **78**(8), 086105 (2007).
39. P. F. Moulton, "Spectroscopic and laser characteristics of Ti:Al2O3," J. Opt. Soc. Am. B **3**(1), 125–133 (1986).
40. P. Albers, E. Stark, and G. Huber, "Continuous-wave laser operation and quantum efficiency of titanium-doped sapphire," J. Opt. Soc. Am. B **3**(1), 134–139 (1986).
41. Y. Li, I. Duncan, and T. Morrow, "Absolute fluorescence quantum efficiency of titanium-doped sapphire at ambient temperature," J. Lumin. **52**(5-6), 275–276 (1992).
42. K. Beha, A. Batalov, N. B. Manson, R. Bratschitsch, and A. Leitenstorfer, "Optimum Photoluminescence Excitation and Recharging Cycle of Single Nitrogen-Vacancy Centers in Ultrapure Diamond," Phys. Rev. Lett. **109**(9), 097404 (2012).
43. O. Svelto, *Principles of Lasers* (Springer, 1998).
44. A. T. Collins, M. F. Thomaz, and M. I. B. Jorge, "Luminescence decay time of the 1.945 eV centre in type Ib diamond," J. Phys. C Solid State Phys. **16**(11), 2177–2181 (1983).

Optical Materials EXPRESS

45. D. Gatto Monticone, F. Quercioli, R. Mercatelli, S. Soria, S. Borini, T. Poli, M. Vannoni, E. Vittone, and P. Olivero, "Systematic study of defect-related quenching of NV luminescence in diamond with time-correlated single-photon counting spectroscopy," Phys. Rev. B **88**(15), 155201 (2013).
46. G. Liaugaudas, G. Davies, K. Suhling, R. U. A. Khan, and D. J. F. Evans, "Luminescence lifetimes of neutral nitrogen-vacancy centres in synthetic diamond containing nitrogen," J. Phys. Condens. Matter **24**(43), 435503 (2012).
47. J. Storteboom, P. Dolan, S. Castelletto, X. Li, and M. Gu, "Lifetime investigation of single nitrogen vacancy centres in nanodiamonds," Opt. Express **23**(9), 11327–11333 (2015).
48. H. Hanzawa, Y. Nisida, and T. Kato, "Measurement of decay time for the NV centre in Ib diamond with a picosecond laser pulse," Diamond Related Materials **6**(11), 1595–1598 (1997).
49. N. B. Manson and R. L. McMurtrie, "Issues concerning the nitrogen-vacancy center in diamond," J. Lumin. **127**(1), 98–103 (2007).
50. A. Batalov, C. Zierl, T. Gaebel, P. Neumann, I. Y. Chan, G. Balasubramanian, P. R. Hemmer, F. Jelezko, and J. Wrachtrup, "Temporal Coherence Of Photons Emitted by Single Nitrogen-Vacancy Defect Centers in Diamond Using Optical Rabi-Oscillations," Phys. Rev. Lett. **100**(7), 077401 (2008).
51. N. Aslam, G. Waldherr, P. Neumann, F. Jelezko, and J. Wrachtrup, "Photo-induced ionization dynamics of the nitrogen vacancy defect in diamond investigated by single-shot charge state detection," New J. Phys. **15**(1), 013064 (2013).
52. B. Aull and H. Jenssen, "Vibronic interactions in Nd:YAG resulting in nonreciprocity of absorption and stimulated emission cross sections," IEEE J. Quantum Electron. **18**(5), 925–930 (1982).
53. F. Träger, *Springer handbook of lasers and optics* (Springer New York, 2007).

1. Introduction

Diamond has a range of properties that make it interesting for laser engineering. The thermal conductivity of pure diamond (2200 W/m K [1]), its rigidity (Young's modulus ~1100 GPa) and tensile strength (2.8 GPa) are significantly superior to commonly used laser gain materials [1, 2]. Even at moderate impurity levels these values remain large with the thermal conductivity of type Ib diamond, the base material used in this study, being reduced by only about 10% [3]. This gives diamond the potential to help alleviate the thermal issues that often limit the performance of solid-state lasers [4], particularly in compact formats. Rapid progress in the growth of high optical quality synthetic diamond [2] makes it important to characterise the laser related properties of this material.

These recent improvements in growth have underpinned significant strides across the field of diamond photonics [5]. Specifically in laser engineering, the availability of high-purity, single-crystal material with low birefringence and low absorption has enabled the routine intra-cavity use of diamond within lasers. Intracavity use of diamond heat spreaders to cool semiconductor disk lasers, for example, has been instrumental in the demonstration of broad spectral coverage at Watt-level output powers from these lasers [4, 6]. However, it should be possible to more fully exploit the exceptional thermo-mechanical properties of diamond if it is used directly as a laser gain material [4]. This has been demonstrated in Raman lasers [7], where stimulated Raman scattering, rather than conventional stimulated emission drives laser oscillation. Output powers from diamond Raman laser are rapidly increasing as the technology develops and better exploits the potential of diamond [8]. While diamond Raman lasers have considerable potential, they would be complemented by a diamond laser technology based on stimulated emission.

In solid-state laser engineering, a laser crystal is usually doped with rare-earth or transition metal ions to enable optical amplification via stimulated emission. Doping of diamond with laser ions is challenging due to the compact nature of the diamond lattice and the relatively large size of laser ions. Doping with ions of similar size to common laser ions has been achieved for non-laser-related applications (see e.g [9]) and there has been discussion of doping for laser applications in the patent literature [10]; however, the optical properties of such material remain unclear, and to the best of our knowledge, laser action has not been reported in the peer-reviewed literature.

A more promising alternative may be to exploit the various colour centres (CC) that can be generated in diamond. A detailed study of hundreds of CCs in diamond can be found in [11]. In contrast to many CC used for laser amplification in other crystals, CC in diamond are often stable and strongly luminescent at, and often significantly above, room temperature. A room temperature diamond CC laser was demonstrated in 1985 [12], based on the H3 CC (two substitutional nitrogen atoms adjacent to a vacancy). However,

Optical Materials EXPRESS

since then no significant progress on diamond CC lasers has been reported. That said, the recent rapid improvements in diamond growth and improved understanding of diamond CC for quantum applications [5] suggests that renewed study may be merited.

One of the most common impurities in synthetic diamond is single substitutional nitrogen, which is incorporated in the diamond lattice substituting a carbon atom [13]. When substitutional nitrogen is adjacent to a vacancy in the diamond lattice, it forms the nitrogen-vacancy (NV) CC [13]. The negatively charged variant of this CC, NV- [14, 15], is particularly well studied since its quantum properties are suitable for applications such as quantum information processing, single-photon sources and optical magnetometry [16].

While there has been considerably less work on NV- for laser applications, a theoretical study predicted the potential for using laser action in NV- for magnetometry with $fT/(Hz)^{1/2}$ sensitivity [17, 18], and recently an observation of stimulated emission in NV- in diamond was reported [19]. It has also been proposed that NV CC may possess promising properties for tunable solid-state lasers [20] in the visible spectral region: a luminescence bandwidth of ~120 nm and peak emission cross-section of $3.2\text{x}10^{-16}$ cm^2 were reported when pumped at 532 nm [21].

NV CC in the neutral charge state (NV0) are less widely studied. However, this CC exhibits broadband luminescence (~550-750 nm [15]) at slightly shorter wavelengths than NV-, and hence is also potentially of interest for tuneable and ultrafast visible laser applications. Other common impurities in diamond include the so-called A (two nitrogen atoms next to each over) and B aggregates (two combined A centres), and Boron impurities [22].

In this paper, we present a detailed study of the laser-related spectroscopic properties of diamond containing NV0 and NV- CC. The next section outlines the samples studied, with subsequent sections describing measurements of the luminescence quantum yield, the luminescence lifetime, and the emission cross-section. Finally, this data is used to estimate the likely gain spectra of these samples to assess the potential for future laser operation.

2. Sample selection, fabrication and characterization

In quantum applications, isolated NV centres are typically required, and so single centres, or samples with low CC concentration, are most often studied. For bulk laser applications, in contrast, ensembles of large numbers of centres will be required to enable efficient optical pumping. The sample sizes and centre densities required can be estimated, to first order at least, by considering the requirements for efficient pump absorption, a prerequisite for efficient laser operation.

Assuming optical pumping of NV- CC by a 532 nm laser, one can estimate the pump power absorbed as a function of CC density and sample length. For a sample with an NV- density of N_{NV^-} and a length L, the fraction of pump power absorbed will be $1 - exp(-\sigma_{abs}N_{NV^-}L)$, where σ_{abs} is the absorption cross section of NV- at 532 nm (reported to be 3.1×10^{-17} cm^2 [23]). Single crystal diamond samples of high optical quality are typically restricted to a few mm in length, and >50% pump absorption would typically be desired for laser applications. Hence, assuming a 2 mm long crystal (a typical length of a reasonably priced high quality synthetic diamond) and targeting a pump absorption of at least 50% at 532 nm, the required concentration of NV- is ~1×10^{17} cm^{-3} or ~0.6 parts per million (ppm) (1 ppm in diamond corresponds to a concentration of 1.77×10^{17} cm^{-3}). For this reason CC concentrations in the region of 1 ppm were targeted in this work.

Two synthetic diamond samples have been studied, labelled below as E6NV and E6H3D (see Fig. 1). Both samples were grown by chemical vapour deposition (CVD) by Element Six Ltd. CCs in sample E6NV were fabricated by Element Six (UK) Ltd.: the crystal was electron irradiated at 4.5 MeV with the total electron dosage of 5.85×10^{18} e/cm^2 then annealed at 400 °C for 2 hours (to anneal out interstitial carbon), 800 °C for 16 hours (to create NV- CC) and 1200 °C for 2 hours (to remove vacancy chains) [24, 25] and studied as received. Sample E6H3D was subjected to treatment by the authors to modify its CC content.

Optical Materials EXPRESS

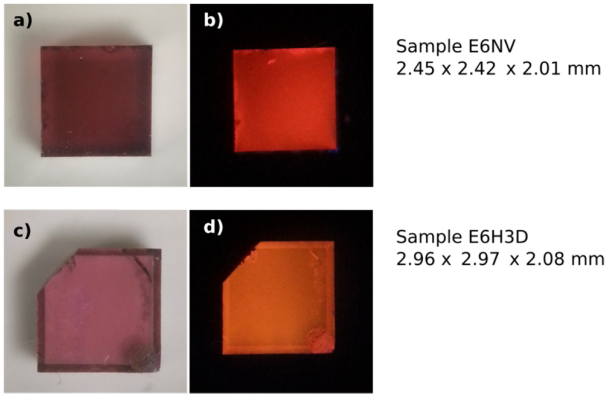

Fig. 1. Sample E6NV under white light a) and UV illumination b). Sample E6H3D under white light c) and UV illumination d).

Prior to further treatment, the room temperature absorption spectrum of sample E6H3D was characterized in the UV-visible region (see Fig. 2, measured with an Agilent Cary 5000 UV-Vis-NIR spectrometer). Negligible absorption was observed in the spectral region above 500 nm; the absorption band at ~267 nm is associated with single substitution nitrogen [3]. This sample had an NV- concentration of <10 ppb (parts per billion) and an H3 concentration of 0.05 ± 0.015 ppm, based on the low temperature absorption spectrum (calculated using the calibration constants and methodology in [26]). The concentration of single substitutional nitrogen (Ns0) in this sample was estimated to be 7 ± 1 ppm from the Fourier transform infrared (FTIR) spectrum measured using a Perkin Elmer Spectrum-GX instrument and the methodology described in [27]. This makes it potentially suitable for generating ppm levels of NV centres without excessive residual single nitrogen.

In order to create NV centres in this crystal, it was subjected to electron beam irradiation and high temperature annealing. Electron irradiation creates vacancies in the diamond lattice [28]. Annealing mobilizes these vacancies such that some can combine with Ns0 to form NV [29, 30]. The charge state of the NV is dependent on the concentration of electron donors in the lattice. These can be, for example, residual Ns0 [31].

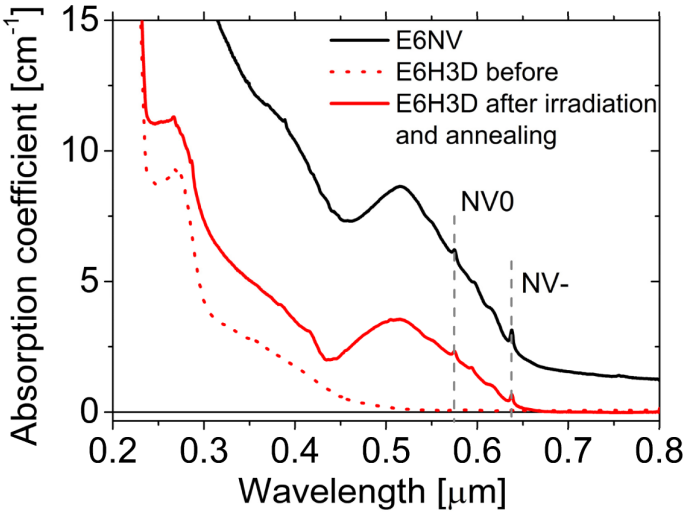

Fig. 2. Room temperature unpolarised absorption spectra for sample E6NV and E6H3D.

Optical Materials EXPRESS

If, for the purposes of an initial estimate of the required electron dose, it is assumed that all generated vacancies combine with Ns0 to create an NV centre, then the required concentration of vacancies is the same as the required NV centre concentration (N_{NV}). If, for a given energy, one electron creates A vacancies within its stopping distance L, the required electron dosage per unit area is $X = N_{NV} \cdot L/A$. Electrons with an energy of 4.5 MeV have a stopping distance in diamond of ~7.5 mm [32]. A beam with this energy creates ~2 vacancies per electron [32]. Therefore, given the estimate of the required NV concentration calculated above (~1 ppm), the corresponding electron dosage would be ~1 × 10^{17} e/cm^2.

In order to generate NV- centres in preference to NV0, it is typical to target an NV concentration that is less than half of the nitrogen concentration, so that an electron can be donated from a nitrogen to an NV centre to form NV- [33]. In E6H3D this requirement is fulfilled: the targeted NV concentration (~1 ppm) is less than half of the total (7 ± 1 ppm) concentration of nitrogen.

Electron irradiation of the sample was performed with an electron density of 1.6 × 10^{17} e/cm^2 and an electron energy of 4.5 MeV. This density was higher than the estimate given above since, in practice, not every vacancy will combine with a nitrogen. An annealing temperature of 800 °C and annealing time of 5 hours were chosen based on the recommendations in [34].

The UV-VIS room-temperature absorption spectra of E6H3D before and after treatment and that of E6NV are presented in Fig. 2. The spectra are characterized by narrow peaks at 575 nm and 637 nm, associated with the zero phonon lines (ZPLs) of NV0 and NV- [11, 29] and the corresponding phonon sidebands with a maximum absorption at ~520 nm.

Absorption spectra at 77K (Fig. 3, measured with a Perkin Elmer Lambda 1050 UV-VIS spectrometer) show defined ZPLs, which can be used to estimate the concentration of NV0, NV- and H3 CC in the samples. It should be noted that spectral position of ZPL of H3 CC (503.2 nm [11]) is very close to the one of the 3H CC (a vacancy-interstitial defect [35]) at 503.4 nm [11]. However, the latter is believed to disappear during long annealing time at temperatures above 600 K [36]. Therefore we considered the observed low-temperature absorption peak at ~503 nm (Fig. 3) as the one corresponding to H3 CC. Sample E6NV also exhibits some well-defined ZPLs at ~727, 712, 693 and 663 nm. The 727 nm peak can be associated with the Ni defects in diamond [11]. The nature of other lines in the absorption spectrum is not well understood, although their presence in diamond was reported in [11].

Concentrations of Ns0, estimated from the FTIR spectroscopy in sample E6H3D after treatment and sample E6NV, were 4 ± 1 and 1.5 ± 0.5 ppm respectively. The combined concentration of A and B aggregates in sample E6NV was found to be higher (5 ± 1 ppm) than that in sample E6H3D after the treatment (3.5 ± 0.5 ppm). The higher background absorption at wavelengths longer than 650 nm in E6NV may be associated with these aggregates, as well as with some absorption associated the absorption centres noted above.

Concentrations of NV0, H3 and NV- CC are proportional to the area under the respective ZPLs in Fig. 3 and are calculated using the calibration constants in [26]. The resulting estimated concentrations are shown in Table 1. No ZPLs associated with neutral vacancies (V0) at 741 and 744 nm [11] were observed in sample E6H3D (see Fig. 3), suggesting any remaining vacancies in the sample were annealed off. The absorption spectrum of sample E6H3D after irradiation (before the annealing) was not measured by us. However, judging from the absorption data of two comparable samples which were treated with the same irradiation dose, we expect to have created about 0.8 ppm of V0. This number agrees well with the total number of H3 and NV CC of 0.8 ppm after annealing (Table 1).

Optical Materials EXPRESS

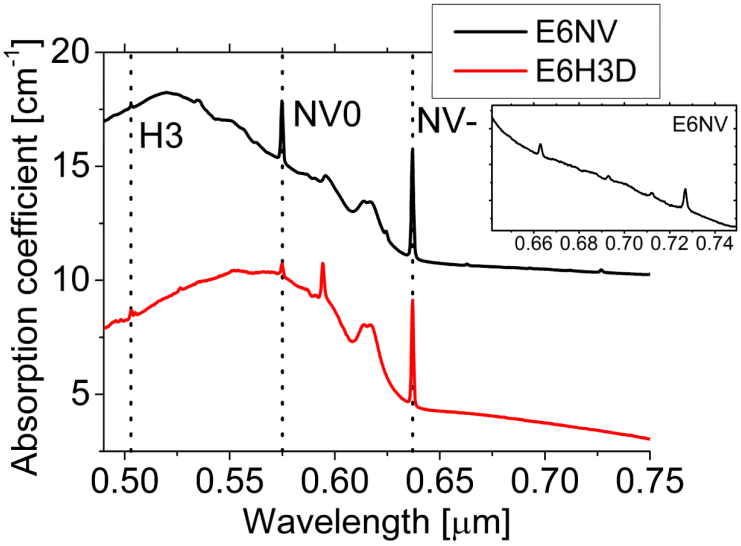

Fig. 3. Absorption spectra of samples E6NV and E6H3D, taken at 77 K.

Table 1. Defect concentrations in samples estimated by the integrated ZPLs in absorption measurements taken at 77K

	Concentrations [ppm]		
Sample	NV0	NV-	H3
E6NV	0.73±0.18	0.55±0.14	0.04±0.015
E6H3D	0.19±0.05	0.50±0.13	0.11±0.04

The absorption cross sections of NV- and NV0 CCs at corresponding ZPLs (637 and 575 nm) can be estimated from the concentration data (Table 1) and the amplitude of low-temperature absorption coefficients at corresponding ZPLs (Fig. 3), after subtracting the background absorption. The absorption cross-section of NV- CC at 637 nm was calculated to be $(4 \pm 1) \times 10^{-17}$ cm^2, and that of NV0 to be $(1.8 \pm 0.4) \times 10^{-17}$ cm^2 at 575 nm.

The concentrations of NV- in samples E6H3D and E6NV are similar at around 0.5 ppm (Table 1). However, a significantly higher concentration of NV0 in sample E6NV (0.7 ppm) results in stronger absorption in the phonon side band at ~520 nm in comparison with that of the sample E6H3D after treatment (Fig. 2).

3. Luminescence spectra and quantum yield measurements

To help establish the potential of the diamond samples for laser operation, luminescence spectra and quantum yield (QY) measurements were made. An integrating sphere (Thorlabs IS200) was used to collect the luminescence from the samples. A spectrometer (Ocean Optics, S2000) was connected to the detector port of the integrating sphere using a multi-mode fibre. The spectral sensitivity of the detection system was calibrated using a tungsten lamp (Ocean optics, HL-2000-FHSA) with a known spectrum (provided by the manufacturer).

The samples were pumped through one of the input ports of the integrating sphere using CW lasers at 447 nm (diode laser, LRD-0447, Laserglow) and 532 nm (solid-state laser, FCHPG-5000, Elforlight). The laser power incident on the samples was 15 mW in both cases. The samples were suspended inside the integrating sphere using a piece of white thread glued to the surface of the sample on one side and to the end cap of the integrating sphere on the other.

The luminescence QY (Φ) of the samples was measured using a comparison method, described in detail in [37], and was calculated with the following equations [38]:

Optical Materials EXPRESS

$$\Phi = \frac{\Phi_x}{1 - a + a \cdot \Phi_x} \tag{1}$$

$$\Phi_x = Q_s \cdot \frac{A_x}{A_s} \cdot \frac{1 - T_s}{1 - T_x} \cdot \left(\frac{n_x}{n_s} \right)^2 \tag{2}$$

where Φ_x, calculated from Eq. (2), is the QY uncorrected for any reabsorption of the luminescence by the emitting centres [37, 38]. Φ_s is the QY of a standard material (Ti:sapphire, which has a reported QY of 0.7 ± 0.1 [39–41], was used in this work); A_x and A_s are the integrated areas under the luminescence spectrum of the sample under study and the standard respectively; T_x (T_s) is the transmittance of the sample under study (standard); n_x (n_s) is the refractive index of the sample under study (standard). The quantity a, set out in Eq. (3), is the self-absorption parameter introduced in [38] to account for the effects of reabsorption [37, 38]:

$$a = 1 - \frac{\int_0^\infty I_x(\lambda) d\lambda}{\int_0^\infty I_{low}(\lambda) d\lambda} \tag{3}$$

In calculating this parameter, it is assumed that the long-wavelength tail of the luminescence spectrum is unaffected by reabsorption and so is independent of the concentration of emitting centres. Therefore the emission spectra of two samples are measured: the spectrum of the sample under test ($I_x(\lambda)$) and the spectrum from a sample with a significantly lower concentration of the emitting centres. The spectrum from the lower concentration sample is then scaled such that its long wavelength tail matches that from the sample under test. This scaled spectrum ($I_{low}(\lambda)$) is then used in Eq. (3) to calculate a, as discussed below.

The measured luminescence spectra of the diamond samples and the Ti:sapphire crystal, pumped at 532 and 447 nm and corrected for spectral sensitivity of the detecting system, are presented in Figs. 4(a) and 4(b). To calculate a (Eq. (3)), the spectrum of a sample with an NV- concentration that is at least 50 times lower than that of the other samples, and a NV0 concentration at least 6 times lower, (ADCVD, N_{NV0} = 0.03 ppm, N_{NV-} <0.01 ppm) was measured at both pump wavelengths. Examples of the luminescence spectra of the lower concentration sample after the procedure of matching the long-wavelength tail of higher concentration samples are shown in Figs. 4 (a) and 4 (b): Fig. 4 (a) for a pump wavelength of 532 nm and sample E6H3D, and Fig. 4 (b) for a pump wavelength of 447 nm and sample E6NV. The results of the measurements are summarised in Table 2 (the error bounds in the table include both standard deviation and systematic errors).

Optical Materials EXPRESS

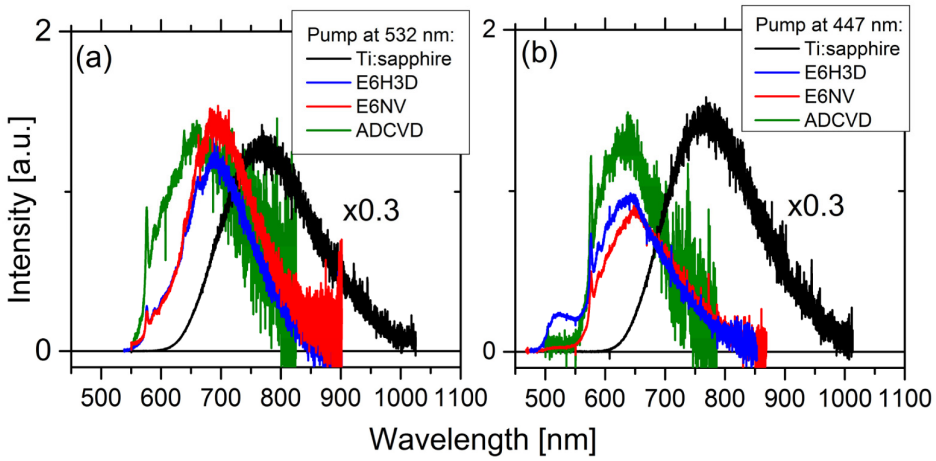

Fig. 4. Luminescence spectra of the diamond samples and Ti:sapphire crystal pumped at 532 nm (a) and at 447 nm (b) measured using an integrating sphere. Examples of the matching the long-wavelength tail of the emission spectra (rescaled) from the low-concentrated sample (ADCVD, green lines) to that of the samples E6H3D (a) and E6NV (b) are also shown.

Table 2. Results of quantum yield measurements

Sample	Pump Wavelength					
	447 [nm]			532 [nm]		
	Φ_x	a	Φ	Φ_x	a	Φ
E6NV	0.13 ± 0.06	0.25	0.17 ± 0.06	0.32 ± 0.1	0.3	0.4 ± 0.1
E6H3D	0.25 ± 0.1	0.17	0.28 ± 0.1	0.4 ± 0.1	0.24	0.48 ± 0.1

The luminescence spectra obtained for the diamond samples is affected not only by reabsorption effects, however, but also by the balance of CC excited by a particular pump wavelength. For example, at the pump wavelength of 532 nm, both NV0 and NV- CC are excited [42] and the contribution of these CC to the luminescence spectrum will depend on their relative concentration, which is different in the samples under study and the low concentration sample. At the pump wavelength of 447 nm both H3 and NV0 CC are excited [42]. Relatively high concentrations of H3 in sample E6H3D means that emission from this defect is more pronounced in the spectra from this sample that those from E6NV. Emission from H3 CC in E6H3D can be seen as a characteristic shoulder in the luminescence spectrum (Fig. 4(b)) at ~510 nm. This will affect the accuracy of the parameter a for the studied diamond samples

Moreover, given that the pump light is typically absorbed by more than one CC, it is difficult to determine correctly the transmittance T_x of the specific CC to use in Eq. (2). Hence the QY values in Table 2 are best interpreted as the ones for the sample as a whole, with some correction for reabsorption by the emitting centre but not for absorption by other centres. They are not, therefore, measurements of the QY of a particular CC but rather of the ensemble of centres in the sample. Sample E6NV has a QY of 0.17 for pumping at 447 nm, rising to 0.4 for pumping at 532 nm. For sample E6H3D these values are 0.28 and 0.48 respectively.

4. Luminescence lifetime measurements

Luminescence lifetime is an important laser parameter, helping to dictate, for example, the laser threshold [43]. Luminescence lifetime measurements were made on the samples at room temperature using a time-correlated single photon counting spectrometer (Edinburgh Instruments Mini-Tau). Two pump sources were used: a 448 nm diode laser with an average power of 0.12 mW and pulse duration of 128 ps (20 MHz repetition rate); and a 562 nm light emitting diode with an average power of 0.09 μW and a pulse duration of 1.5 ns (10 MHz repetition rate). The lifetime measurements were spectrally gated to wavelengths around 640, 670 and 700 nm (using filters with a pass band of 10nm, full-

Optical Materials EXPRESS

width at half-maximum), as well as in the spectral range >640 nm (using a long-pass filter). The filters blocked >99.99% of light out of the bandpass spectral region. The first band corresponds to the ZPL of NV-, the second to the maximum of the NV- phonon sideband, and the third to the long-wavelength tail of the NV- the luminescence spectrum. The measurements at >640 nm were carried out for comparability with those in [44].

The typical luminescence decay kinetics are shown in Fig. 5 for the spectral range > 640 nm. For 448 nm pumping, the luminescence decay is mono-exponential with a decay time of 20-22 ns at all emission wavelength bands measured and for both samples.

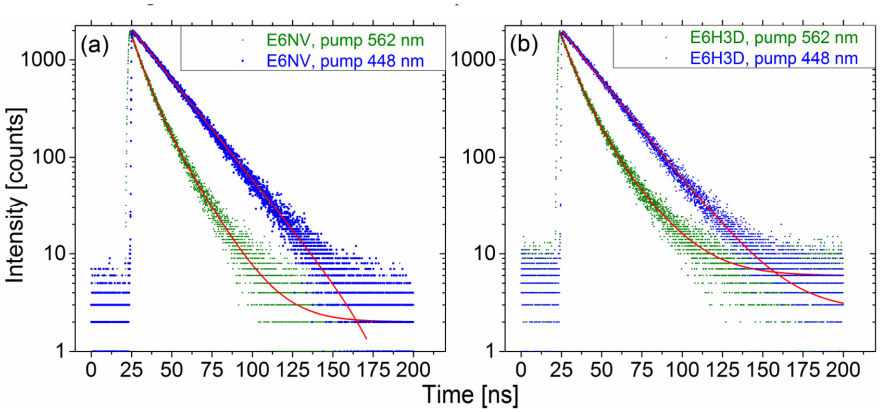

Fig. 5. Luminescence decay of the samples E6NV (a) and E6H3D (b) at emission wavelengths >640 nm at the pump wavelengths of 448 and 562 nm: dots - experimental results, solid lines - best fits using single- (pump wavelength 448 nm) and double- (pump wavelength 562 nm) exponential decay models.

For 562 nm pumping, the luminescence decay had double exponential kinetics for all emission wavelength bands measured. The summary of the fitting of the experimental data with the double-exponential decay function $I_0 + A_f \cdot exp(-t/\tau_f) + A_s \cdot exp(-t/\tau_s)$ is presented in Table 3. In general, the fast (τ_f) component lifetime was between 7 and 9 ns, and the slow (τ_s) component was between 17 and 21 ns. The one exception was the measurement of sample E6NV, where the slow component was ~16 ns.

Table 3. Results of luminescence lifetime measurements in diamond samples

Sample		E6NV				E6H3D			
λ_{pump} [nm]	λ_{lumin} [nm]	A_{sl}	τ_{sl} [ns]	A_f	τ_f [ns]	A_{sl}	τ_{sl} [ns]	A_f	τ_f [ns]
488	640		20				20		
	670		20				22		
	700		20				22		
	>640		21				21		
562	640	921	17.5	1029	7.2	910	20.6	1108	8.9
	670	604	17.2	1321	7.7	633	19.3	1288	8.2
	700	457	17.5	1418	8	499	19.1	1424	8.2
	>640	660	15.9	1254	7.1	501	19.4	1418	8.3

We attribute the difference in the luminescence decay kinetics at pump wavelengths of 448 and 562 nm to different CC being excited: mainly NV0 at 448 nm and both NV- and NV0 at 562 nm, based on the photoluminescence excitation spectrum measurements reported in [42]. The measured luminescence decay time for the 448 nm pump is encompassed by the previously reported values of the luminescence lifetime of NV0 (17-28 ns [42, 45–47]).

Collins et al. reported a radiative lifetime of 13 ± 0.5 ns for NV- [44]. This was measured in natural diamond at a pump wavelength of 580 ± 20 nm and for an emission spectral range of >640 nm. It didn't vary significantly over a temperature range of 77 to 700 K. Hanzawa et al reported bi-exponential luminescence decay in synthetic diamond containing NV CC [48]. The sample was pumped at 587 nm, and fast and slow components of 2 and 8 ns were attributed to NV CC but without attribution to particular

Optical Materials EXPRESS

charge states. Manson et al. [49] showed that, under certain circumstances, bi-exponential decay could result from the different lifetimes for the spin-projection states $m_s = 0$ and $m_s = \pm 1$. However, they predicted that the fast component (associated with $m_s = \pm 1$) should only be observed for low repetition rate pumping (< 10 Hz), or when the spin polarisation is removed with a microwave (MW) field. The latter condition was realised in [50], where fast and slow decay times of 7.8 and 12 ns were measured.

The repetition rate used in our measurements was 5 MHz. Hence, in the absence of a microwave field, the bi-exponential luminescence decay observed at a pump wavelength of 562 nm is likely to be due to two different CC being excited: NV- and NV0. The amplitude of the slow component (A_{sl}) decreases as the emission wavelength examined is shifted from 640 to 700 nm, while that of the fast component (A_f) increases (Table 3). This is consistent with sampling close to the peak of the phonon sideband for NV0 (640 nm) to sampling close to the peak of the phonon sideband for NV- (700 nm) and hence preferentially sampling NV0 at 640 nm and NV- at 700 nm.

The evidence suggests that the fast and slow components of the luminescence decay can be assigned to NV- and NV0 CC, respectively. Shorter luminescence lifetimes of NV0 CC, detected at the pump wavelength of 488 nm in comparison with that at 562 nm (Table 3, column τ_{sl}) could be attributed to non-radiative energy transfer mechanisms (e.g. photo-ionisation [51]) in NV0 CC taking place at pump wavelength of 562 nm.

The measured luminescence lifetimes for NV- of ~7.5 ns in sample E6NV and ~8.3 ns in E6H3D are shorter than the reported radiative lifetimes of ~13 ns [44]. This is likely to be due to non-radiative relaxation channels resulting from defect related quenching [44, 45]. The luminescence QY of NV- in the samples can be estimated from the ratio of the luminescence and radiative lifetimes [43]. If a radiative lifetime of 13 ns is assumed [44], then QYs of 0.58 and 0.64 can be estimated for samples E6NV and E6H3D, respectively.

To the best of the authors' knowledge, no direct measurements of the radiative lifetime of NV0 in diamond have been published. However, some indirect measurements (based on the results of luminescence kinetics in what was believed to be optically pure CVD diamonds, pumped at ~0.45 μm) [45, 46] suggest that the "intrinsic" or radiative lifetime in NV0 CC is 17 ± 1 [45] or 19 ± 2 ns [46]. Given that the luminescence lifetimes measured in this work are similar to, if not longer than, the previously quoted estimates of the radiative lifetime, it may be that the QY of NV0 in these samples is approaching 100%.

The QY of NV- CC was reported to be 100% in [11], however no information was given on the methods used to determine this value. As far as NV0 CC is concerned, to the best of the authors' knowledge, there are no report on QY measurements in this centre.

The difference between the results returned by the two QY measurement techniques (integrating sphere in Section 3 and luminescence lifetime in this Section) indicates relatively strong absorption of the pump light by centres other than the target centre, in particular Ns0, and is affecting the QY results returned by the integrating sphere method (Section 3).

5. Stimulated emission cross-section

The stimulated emission cross sections of NV CC in our samples were calculated using the Füchtbauer-Ladenburg equation. This method requires knowledge of the radiative lifetime and a measured luminescence spectrum [52]. The emission cross section $\sigma_{em}(\lambda)$ is related to the luminescence intensity $I(\lambda)$ by [53]:

$$\sigma_{em}(\lambda) = \frac{\lambda^5}{\tau_r \left(\int \lambda I(\lambda) d\lambda\right) 8\pi n^2 c} I(\lambda) \tag{4}$$

where τ_r is the radiative lifetime, λ is the wavelength and n the refractive index for diamond, c is the speed of light. To calculate the emission cross-section of NV-, the luminescence spectra of the samples pumped at 532 nm was corrected for the contribution of emission from NV0 (similar to a procedure, described in [19]). To do this correction, the luminescence spectra of the samples pumped at 447 and 532 nm were recorded.

Optical Materials EXPRESS

Whereas the emission spectrum for 532 nm pumping results from both NV0 and NV- emission, the spectrum pumped at 447 nm is dominated by NV0. Both spectra were normalized to the intensity of the zero phonon line of NV0 at 575 nm, and the normalised spectrum for 447 nm pumping was then subtracted from normalised spectrum for 532nm pumping. This procedure was carried out for both E6NV and E6H3D samples and the result for sample E6NV is shown in Fig. 6 (a) (the result for sample E6H3D is similar).

The luminescence spectrum of the sample E6H3D after treatment, pumped at 447 nm, is a result of emission of both NV0 and H3 CC. In the case of sample E6NV, the contribution of H3 CC to the luminescence under 447 nm pumping is less intense, see Fig. 4. For this reason, in order to calculate the emission cross-section of NV0 CC in sample E6H3D, its luminescence spectrum, pumped at 447 nm was corrected for contribution of emission from H3. To do this correction, the luminescence spectra of the sample, before and after the treatment and pumped at 447 nm, were recorded. The spectrum for the untreated sample is dominated by H3 CC (due to very low concentrations of NV- CC). Both spectra were normalized to the intensity of the zero phonon line of H3 at 503 nm, and the normalised spectrum of untreated sample was then subtracted from normalised spectrum the treated one. The result of this procedure is shown in Fig. 6 (b). These corrected spectra were then used with Eq. (4).

The calculated stimulated emission cross section spectra for NV- as a function of wavelength are plotted in Fig. 7 for both samples, taking into account the radiative lifetime of NV- CC of 13 ± 0.5 ns [44]. The peak emission cross-section is estimated to be $\sigma_{em} = (3.6 \pm 0.1) \times 10^{-17}$ cm^2 at 710 nm for both samples.

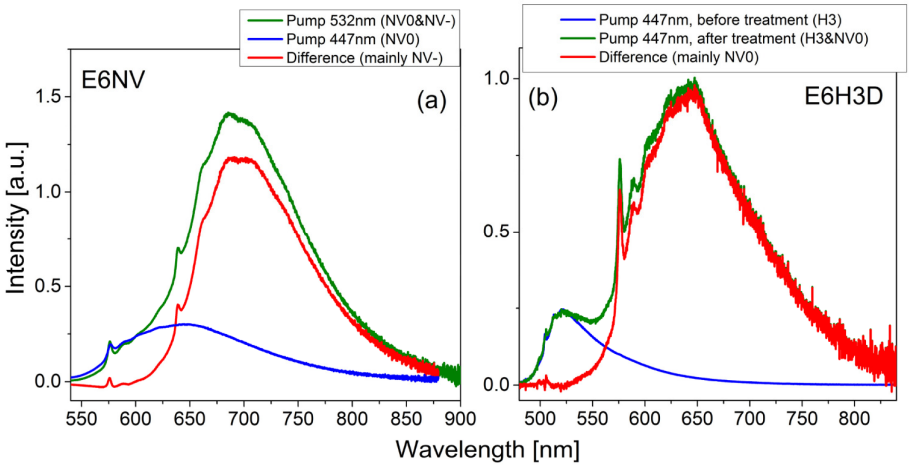

Fig. 6. Results of correction of the luminescence spectra of diamond samples pumped at 532 (a) and 447 nm (b) for contribution of emission from NV0 (a) and H3 CC (b).

Optical Materials EXPRESS

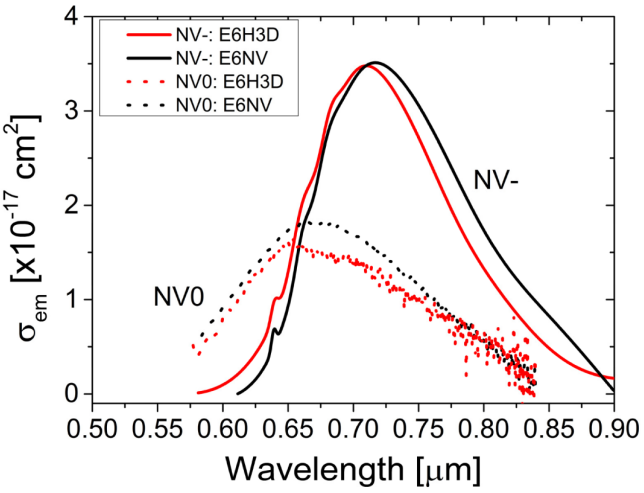

Fig. 7. The emission cross sections of NV- and NV0 CC ($\sigma_{em,}$) for samples E6NV and E6H3D calculated using Eq. (4). The difference in the shape of the cross section spectra is attributed to the difference in CC concentration and its contribution to the luminescence spectra.

This value is ~8 times smaller than the one estimated in Vins et al [21]. However, the charge state of the NV centres was not discussed in [21] and the radiative lifetime assumed in the calculation of stimulated emission was not disclosed.

The results of calculations for NV0 CC, taking into account an estimated radiative lifetime of NV0 of 20 ± 1 ns based on our data from Section 3, are also presented in Fig. 7 for samples E6NV and E6H3D. The peak emission cross-section value is in the range 1.6-1.8 × 10^{-17} cm^2 at ~660-670 nm.

6. Calculation of the gain spectrum of NV- and NV0 CC in diamond

The gain spectra can be calculated from the emission and absorption spectra of the samples using the following equation [53]:

$$g = \sigma_{em} \cdot N_{NV} \cdot \beta - \alpha_{abs} \tag{5}$$

where N_{NV} is the total concentration of NV- or NV0 CC in the sample. For the gain calculation in NV- CC we assumed that the main contribution to the absorption of the samples at the wavelengths longer than the ZPL of NV- (638 nm), α_{abs}, is due to background defects not directly associated with the NV- or NV0 CCs (e.g. Ns0). Hence, absorption from these states can be assumed to be independent of the inversion level β of the NV- CC. For the gain calculation in NV0 CC, the background absorption at the wavelengths longer than the ZPL of NV0 (575 nm) is assumed to be associated with both Ns0 and NV- CC. Still, absorption from both of these states can be assumed to be independent of the inversion level β of the NV0 CC.

Calculated gain spectra of NV- and NV0 in the two samples at two inversion levels β of 0.3 and 1 of corresponding CC, are shown in Figs. 8 (a) and 8 (b) respectively, using the absorption spectra measurements in Fig. 2. β of 1 represents an upper bound on the gain, while β of 0.3 is more reasonably achievable, with the required pump intensity of ~0.4 MW/cm^2 for both NV- and NV0 CC. NV- in sample E6H3D shows positive gain in the spectral range between 670 and 820nm for β = 0.3 (Fig. 8), which makes it a promising candidate for laser action. NV0 looks less promising, however. Significant gain in sample E6H3D can only be achieved for an inversion factor β>0.3 and reaches a maximum value of <0.5 cm^{-1} at β = 1 In the case of the sample E6NV the maximum achievable gain is 1.05 cm^{-1}.

Optical Materials EXPRESS

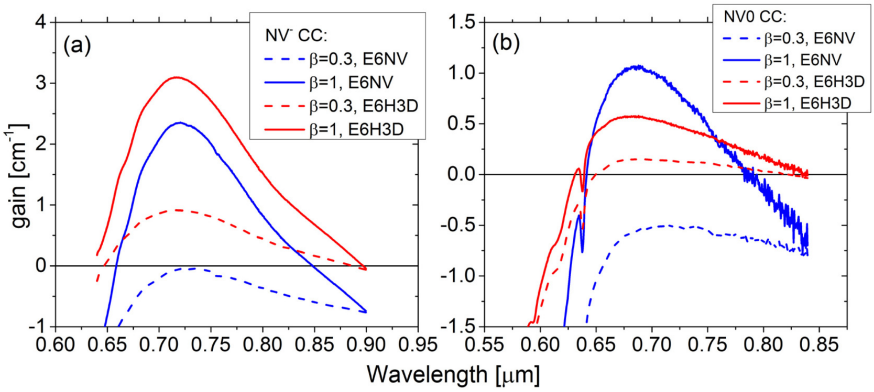

Fig. 8. Calculated gain spectra of NV- (a) and NV0 (b) at the pump wavelength of 532 nm (a) and 447 nm (b) for different inversion factors β and for the two samples under study.

The emission spectrum of an NV- laser (for a pump wavelength of 532nm) or an NV0 laser (for a pump wavelength of 447nm) will be determined by a balance between the gain spectrum (Fig. 8) and any additional passive losses introduced e.g. by the resonator mirrors. The above mentioned pump intensity of 0.4 MW/cm^2 required for a positive gain in both NV- and NV0 CC corresponds to 0.6 W of absorbed pump power for a Gaussian pump spot radius in the crystal of 10 μm, which is achievable using commercial CW lasers. If pumped in the blue (e.g. 447 nm) the NV laser will predominantly operate via the NV0 CC (see Fig. 4 (b)), while with the green pumping (e.g. 532 nm) some cooperative effects from both NV0 and NV- CC can be expected (see Fig. 4 (a)). Further research is required to determine the optimal balance between the initial concentration of Ns0 and the final concentration of NV- and NV0 CC to achieve the highest laser gain with lowest possible background absorption losses.

7. Conclusions

In this paper the key laser-related spectroscopic parameters of NV- and NV0 CC in diamond have been measured in two samples with CC concentrations around the level that might be required for future laser operation (~1 ppm). For the NV- centre, the luminescence lifetime and peak stimulated emission cross-section were measured to be 8 ± 1 ns and (3.6 ± 0.1) × 10^{-17} cm^2 respectively. For NV0, these quantities were 20 ± 1 ns and (1.7 ± 0.1) × 10^{-17} cm^2. The luminescence QY of the samples was also measured in two ways: by collecting the total luminescence using an integrating sphere and by comparing the luminescence lifetime to the radiative lifetime. The former returned the QY of the sample overall, factoring in the effect of absorption by other centres; the latter returned an estimate of the yield of particular centres were there no such absorption. The QY of NV- and NV0 in these samples was relatively high and similar for the two samples: 60% for NV- and approaching 100% for NV0. However, parasitic absorption in the samples meant the QYs from the samples overall were substantially lower: <30% for pumping at 447 nm and <50% for pumping at 532 nm. To further assess the potential for laser operation, the gain spectra for NV- and NV0 were estimated at two inversion levels. These calculations indicated that the NV- centre is more promising at present for future laser engineering than NV0 and that while the centres themselves have intrinsic properties that look promising for laser operation, further work is required on the synthesis process to reduced parasitic absorption. In the case of NV0, this is complicated by the fact that NV- absorbs in the NV0 emission region.

Funding

Funding is gratefully acknowledged from the European Research Council (grant number 278389), Fraunhofer UK Research Ltd., and the Royal Academy of Engineering. All data

Optical Materials EXPRESS

created during this research are openly available from the University of Strathclyde Pure/ KnowledgeBase at http://dx.doi.org/10.15129/9ee6178b-4ce9-4907-8d18-2c40085da6b0

Acknowledgments

The authors are grateful to Richard Balmer and Element 6 (UK) for their comments on the manuscript.